



ARTICLE OPEN

Soluble CD4 effectively prevents excessive TLR activation of resident macrophages in the onset of sepsis

Sheng-yuan Zhang^{1,2,3}, Qiu-ping Xu¹, Li-na Shi^{1,3}, Shih-wen Li¹, Wei-hong Wang¹, Qing-qing Wang¹, Liao-xun Lu⁴, Hui Xiao¹, Jun-hong Wang¹, Feng-ying Li¹, Yin-ming Liang¹, Si-tang Gong⁵, Hao-ran Peng⁶, Zheng Zhang¹ and Hong Tang^{1,7}

T lymphopenia, occurring in the early phase of sepsis in response to systemic inflammation, is commonly associated with morbidity and mortality of septic infections. We have previously shown that a sufficient number of T cells is required to constrain Toll-like receptors (TLRs) mediated hyperinflammation. However, the underlying mechanisms remains unsolved. Herein, we unveil that CD4⁺ T cells engage with MHC II of macrophages to downregulate TLR pro-inflammatory signaling. We show further that the direct contact between CD4 molecule of CD4⁺ T cells or the ectodomain of CD4 (soluble CD4, sCD4), and MHC II of resident macrophages is necessary and sufficient to prevent TLR4 overactivation in LPS and cecal ligation puncture (CLP) sepsis. sCD4 serum concentrations increase after the onset of LPS sepsis, suggesting its compensatory inhibitive effects on hyperinflammation. sCD4 engagement enables the cytoplasmic domain of MHC II to recruit and activate STING and SHP2, which inhibits IRAK1/Erk and TRAF6/NF- κ B activation required for TLR4 inflammation. Furthermore, sCD4 subverts pro-inflammatory plasma membrane anchorage of TLR4 by disruption of MHC II-TLR4 raft domains that promotes MHC II endocytosis. Finally, sCD4/MHCII reversal signaling specifically interferes with TLR4 but not TNFR hyperinflammation, and independent of the inhibitive signaling of CD40 ligand of CD4⁺ cells on macrophages. Therefore, a sufficient amount of soluble CD4 protein can prevent excessive inflammatory activation of macrophages via alternation of MHC II-TLR signaling complex, that might benefit for a new paradigm of preventive treatment of sepsis.

Signal Transduction and Targeted Therapy (2023)8:236

; <https://doi.org/10.1038/s41392-023-01438-z>

INTRODUCTION

Innate immune cells sense microbial pathogen-associated molecular patterns (PAMPs) via pattern recognition receptors (PRRs), which include Toll-like receptors (TLRs), NOD-like receptors (NLRs), C-type lectin receptors (CLRs) and nucleic acid sensors.^{1–3} The recognition upregulates both major histocompatibility complexes (MHC I and II) and co-stimulatory molecules, and secretes inflammatory cytokines, to prime subsequent adaptive immune response for protection.⁴

Hyperinflammation due to excessive activation of innate immune cells, however, leads to pathological alterations and correlates with the morbidity and mortality of infections.⁵ Innate inflammation therefore has to be tightly controlled by a series of negative regulators, at multiple levels, to maintain immunological homeostasis.^{6,7} We established previously that a sufficient amount of naïve T cells is required to dampen the acute innate inflammatory response to betacoronavirus and Gram-negative bacteria infections.^{8,9} To do so, T cells need to make direct cell-cell contact with antigen presenting cells (APC) to suppress their TLR-mediated inflammatory response, but independent of T cell receptor (TCR).⁸ Intriguingly, both effector and memory CD4⁺

T cells can block caspase-1/IL-1 β activation by cell-cell contact with APC that diminishes NLRP3 and NLRC4 inflammasome activation.¹⁰

Sepsis is defined as an initial hyper-inflammatory response to systemic infection associated with a subsequent immune suppression and dysfunction, that can lead to multiple organ failure, secondary infections and mortality.¹¹ The onset of sepsis is characterized by leukocytosis (marked increase in neutrophils and monocytes) in the first 2–4 days, followed by a state of lymphopenia as a result of apoptosis (drastic reduction of B cells, CD4⁺ and CD8⁺ T cells). Failure to restore cell numbers during either the stage of leukocytosis or lymphopenia results in increased mortality.^{12,13} Sepsis patients develop long-term immune impairment due to the reduction in the number and function of different immune cell populations.¹⁴ Patients who survive the early phase of sepsis develop immune suppression, which is characterized by T cell exhaustion, unresolved infection and susceptibility to opportunistic infection, and dysfunctional T cell repertoire.¹³ Compared to the understanding of functional impairment, however, the pro-apoptotic factors that cause T lymphopenia in sepsis and the impact of T lymphopenia to sepsis

¹CAS Key Laboratory of Molecular Virology and Immunology, Institut Pasteur of Shanghai, Chinese Academy of Sciences, Shanghai 210031, China; ²The Third People's Hospital of Shenzhen, Shenzhen 518112, China; ³University of Chinese Academy of Sciences, Beijing 100101, China; ⁴The Laboratory of Genetic Regulators in The Immune System, Xin-xiang Medical University, Xin-xiang, Henan Province 453003, China; ⁵The Joint Center of Translational Medicine, Guangzhou Women and Children's Medical Center and Institut Pasteur of Shanghai, Guangzhou 510623, China; ⁶Department of Microbiology, Naval Medical University, Shanghai 200433, China and ⁷State Key Laboratory for Diagnosis and Treatment of Infectious Diseases, National Clinical Research Centre for Infectious Diseases, Collaborative Innovation Centre for Diagnosis and Treatment of Infectious Diseases, The First Affiliated Hospital, Zhejiang University School of Medicine, Hangzhou 310003, China

Correspondence: Hao-ran Peng (phran@126.com) or Zheng Zhang (zhangzheng1975@aliyun.com) or Hong Tang (h_tang@zju.edu.cn)

These authors contributed equally: Sheng-yuan Zhang, Qiu-ping Xu, Li-na Shi, Shih-wen Li.

Received: 29 August 2022 Revised: 8 March 2023 Accepted: 28 March 2023

Published online: 19 June 2023

remain elusive.¹⁵ T lymphopenia, responding to systemic inflammatory response in the early phase of sepsis,¹⁶ is commonly associated with morbidity and mortality of septic infections.¹⁷ Such an acquired T-lymphopenia also occurs in certain autoimmune diseases and inflammaging process.¹⁸ Critically, insufficient number of naïve CD4⁺ T cells is responsible for the unleashed TLR inflammation with high morbidity and mortality rates.³ CD4 uses its extracellular domain to interact with β_2 -domain of MHC II,^{19,20} and MHC II is required for CD4⁺ T cells to suppress TLR hyperinflammation in APCs.^{8,9} Intriguing enough, MHC II is required to constrain B cell-response to LPS,^{21,22} and decreased expression of HLA-DR in monocytes and macrophages is observed in sepsis patients.²³ Nevertheless, how CD4⁺ T cells signal through MHC II to suppress TLR inflammation in APCs remains unknown.

In this study, we demonstrate that CD4 molecule, either membrane bound or soluble ectodomain (sCD4), is necessary and sufficient to hamper TLR inflammation of APC and protect mice from the lethal septic inflammation. Furthermore, CD4 engagement recruits SHP2 and STING to the intracellular tail of MHC II in lipid rafts, which disrupts MHC II/TLR4 signaling complex, and inhibits TLR4 activation of IRAK1/TRAF6/NF- κ B inflammatory response.

RESULTS

CD4 T-lymphopenia accounted for the morbidity and mortality of sepsis

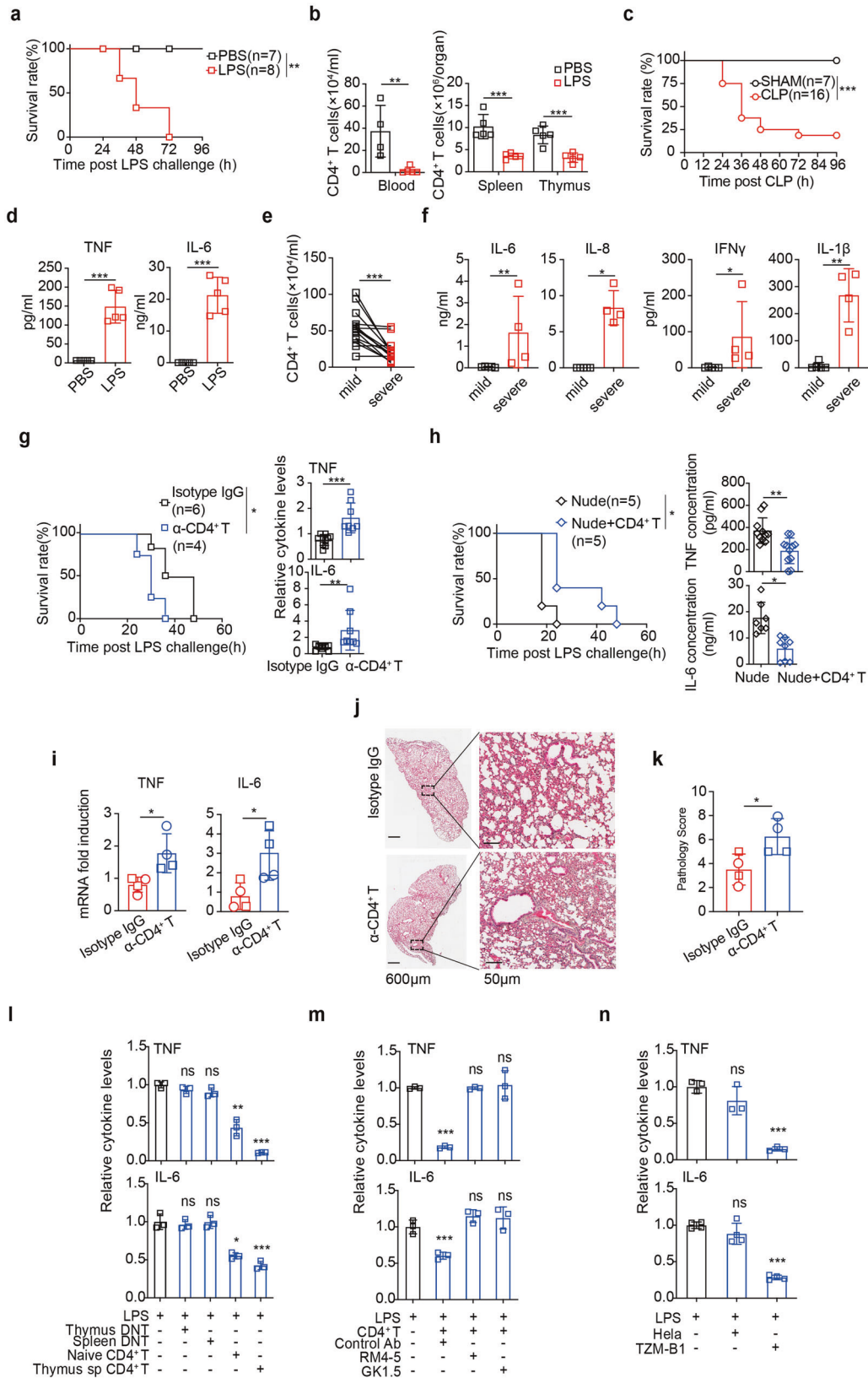
We used LPS endotoxemia in mice as a surrogate of sepsis in patients²⁴ to study the role of CD4⁺ T lymphopenia. C57BL/6 mice succumbed within 72 h post LPS *i.p.* injection (*hpi*, 10 mg/kg, Fig. 1a), accompanied with severe numerical reduction of both CD4⁺ (Fig. 1b) and CD8⁺ T cells (Supplementary Fig. 1a) in the thymus and periphery at 12 *hpi*, with the thymus drastically shrunk (Supplementary Figs. 1b, 2a–b). CD4⁺ T cells were more prone to sepsis-induced apoptosis, shown by reduced ratios of CD4/CD8 T cell counts in the thymus and spleen, as compared to the sham mice (Supplementary Fig. 1c). T lymphopenia was also observed in septic infection of mice by oral gavage of *Salmonella typhimurium* SL1344 (Supplementary Fig. 1d). To substantiate that LPS sepsis induced T lymphopenia can recapitulate that in the classical cecal ligation and puncture (CLP) sepsis (Fig. 1c), we compared side-by-side two models in the first 24 h after treatment. Both models showed qualitatively and quantitatively similar reduction of thymic sizes (Supplementary Fig. 2a) and increased pathology scores (Supplementary Table 4), as reflected by decreased thymocyte numbers, abnormal proportion of medulla and cortex and increased cell death (Supplementary Fig. 2b, c). Both models showed similar tendencies of T cell number reduction, decreased CD4/CD8 ratios except that in thymi of CLP model (Supplementary Fig. 2d,e). These results agreed with the previous CLP results.¹⁵ Therefore, T lymphopenia induced by a septic dose of LPS in mice manifested the dysregulated T cell response in CLP sepsis.

T lymphopenia associated with concomitantly elevated TNF and IL-6 in the serum at 12 *hpi* in LPS sepsis (Fig. 1d) or CLP sepsis (Supplementary Fig. 1e), among other pro-inflammatory cytokines and chemokines (PICC, Supplementary Fig. 1f). During the course of LPS sepsis (0–36 *hpi*), most PICCs reached the first and second peak at 6 and 16 *hpi*, respectively, with IL-6, IL-18, CCL5, CCL7 and CXCL1 sustaining at plateau at 36 *hpi* (Supplementary Fig. 1g). CD4⁺ T lymphopenia in circulation is also a major comorbidity of severe/critical COVID-19 patients who suffer from sepsis.^{25,26} We also observed that the inverse correlation of CD4⁺ (Fig. 1e) and CD8⁺ T cell counts (Supplementary Fig. 1h) and PICC levels (IL-6, IL-1 β , IL-8 and IFN γ) in bronchoalveolar lavage fluids of COVID-19 patients hospitalized in 2020 (Supplementary Table 1), whose symptoms transformed from severe to mild pneumonia after symptomatic treatments (Fig. 1f).

Numerical and functional dysregulation of CD4⁺ and CD8⁺ T cells plays important roles in sepsis onset, progression and recovery.^{12,13} Insufficient number of CD4⁺ T cells per se led to the hyperinflammation and mortality in sepsis, because mice lacking CD4⁺ T cells, either by antibody-ablated (Fig. 1g) or in nude mice (Fig. 1h), were more susceptible to LPS sepsis (poorer survival and higher TNF/IL-6), compared to those by isotype antibody treatment (Supplementary Fig. 1i for antibody depletion efficiency) or CD4⁺ T cells adoptive transfer (Supplementary Fig. 1j for adoptive transfer efficiency), respectively. C57BL/6 mice of CD4⁺ T cells pre-depleted also showed augmented TNF/IL-6 response to SL1344 oral infection (Supplementary Fig. 1k) and much higher bacterial load (Supplementary Fig. 1l). Likewise, antibody depletion of CD4⁺ T cells in K18-hACE2 mice caused higher TNF/IL-6 expression (Fig. 1i) and more severe lung pathology (Fig. 1j, k) 7 d post SARS-CoV-2 infection. Therefore, aside from the functional exhaustion of T cells in the later stage of sepsis, the drastic reduction of CD4⁺ T cell numbers would attribute to the first hit of systemic hyperinflammation of sepsis.

To test critically whether CD4 molecule per se directly mediates CD4⁺ T-cell suppression of LPS/TLR4 inflammation, isolated T cells were co-cultured with bone marrow derived macrophages (BMDM) 2 h before LPS stimulation. T cells lacking CD4, either foreign antigen naïve (thymus DNT) or experienced (splenic DNT), failed to inhibit LPS activated TNF/IL-6 expression, except for naïve or thymic single-positive CD4⁺ T cells (Fig. 1l). Therefore, CD4 moiety of naïve CD4⁺ T cells, but not TCR or TCR restriction as indicated previously,⁸ played an essential role to suppress TLR4 inflammation. This notion was substantiated by the co-culture experiments that anti-CD4 antibodies (RM4-5 or GK1.5) completely prevented CD4⁺ T cells from inhibiting TLR4 inflammation in macrophages (Fig. 1m). Of note, antibodies did not induce CD4⁺ T cell apoptosis (Supplementary Fig. 1m). To exclude the involvement of other CD4⁺ T-cell components, e.g., co-stimulatory receptors, we co-cultured THP-1 cells with TZM-b1 cells, a HeLa derivative that stably expresses human CD4.²⁷ Only TZM-b1, but not HeLa cells, prevented THP-1 cells from TNF and IL-6 response to LPS (Fig. 1n). Collectively, CD4 molecule was necessary and sufficient to restrain TLR4 inflammatory response.

Acute LPS inflammation causes bone marrow (BM) monocytes to rapidly egress into circulation and infiltrate tissues, where they differentiate to inflammatory DCs and macrophages.²⁸ Careful comparison of nude or nude mice adoptively transferred with CD4⁺ T cells (Supplementary Fig. 3a for the partial BM reconstitution) showed that, CD4⁺ T cell deficiency led to more Ly6C^{hi} monocytes retained in BM and less migrated to the blood or infiltrated to the spleen and liver 3 *hpi* (Fig. 2a, Supplementary Fig. 3b for gating strategy). This can be partially explained by the inhibitive effect of CD4⁺ T cells on TLR4 inflammation-driven emergency myelopoiesis in BM (reduced hematopoietic stem cells, common myeloid and granulocyte macrophage progenitors), with megakaryocyte and erythrocyte progenitors intact (Fig. 2b, Supplementary Fig. 3c for gating strategies of hematopoietic lineages). Lack of CD4⁺ T cells also suppressed monocytes activation (Ly6C^{hi} CD64⁺) in BM, the blood, and other indicated peripheral organs (Fig. 2c), likely due to insufficient IFN γ in the absence of CD4⁺ T cells (Supplementary Fig. 3e), as suggested previously.²⁹ These results suggested that CD4⁺ T cells promoted emergency myelopoiesis and monocyte migration to inflamed tissues, necessary for inflammatory leukocytosis. In vitro co-culture experiments showed that CD4⁺ T cells accelerated TLR4-driven BM monocytes differentiation to macrophages, but DC significantly suppressed (Fig. 2d). Indeed, differentiation of spleen/liver-infiltrated monocytes to macrophages (CD11b^{int} F4/80⁺ MHC II⁺, Supplementary Fig. 3d for gating strategies) were increased by CD4⁺ T cells in endotoxemic mice (Fig. 2e), but not the activation of these monocyte-derived macrophages (CD86⁺, Fig. 2f). Surprisingly, the number of resident macrophages (CD11b^{low}F4/



80^{hi}) in the spleen or liver remained unaffected by the presence or absence of CD4⁺ T cells (Fig. 2g), but their activation by LPS was effectively inhibited by CD4⁺ T cells (Fig. 2h). These results would suggest that resident macrophages played a more important role

in mediating hyper-inflammatory response to CD4⁺ T lymphopenia in sepsis. qPCR measurement showed that TNF production was specifically reduced in splenic resident macrophages, but not infiltrated macrophages or monocytes, isolated 3 *hpi* (Fig. 2i).

Fig. 1 Membrane bound CD4 in T cells controlled TLR4 inflammation. **a** Survival rates, **(b)** CD4⁺ T cell counts in the indicated organs, and **(d)** serum TNF and IL-6 were measured 12 h after *i.p.* LPS ($n = 7-8$). **c** Survival rates were measured after CLP ($n = 7-16$). **e** Absolute numbers of peripheral CD4⁺ T cells, **(f)** indicated cytokines of BALF were measured in COVID-19 patients ($n = 15$). Survival rates and TNF/IL-6 levels were measured as in **(a-c)** except that CD4⁺ T cells were **(g)** pre-depleted (GK1.5) for 2 days, or **(h)** supplemented to nude mice for 7 days, before LPS injection. **i-k** hACE2 mice pre-treated with GK1.5 antibody or isotype IgG were infected with SARS-CoV-2 for 7 days. **i** Fold changes of TNF and IL-6 mRNA normalized to *actin* in the lung by qPCR and **(j-k)** representative sections and pathology score of the lobe of left lung (with respective magnifications of areas of interest) on day 7. SARS-CoV-2 virus ($pfu \times 10^2$ in box; $pfu \times 10^5$ in circle). **l, m** Measurement of TNF and IL-6 in supernatants of BMDM 16 h after incubation with LPS (100 ng/mL), in the absence or presence of **(l)** T cells of the indicated origins (macrophages: T cells = 1:1), or **(m)** naive CD4⁺ T cells with the indicated blocking mAb against CD4 (RM4-5; GK1.5). **n** TNF and IL-6 in supernatants 3 h after LPS treatment of THP-1 cells co-cultured with HeLa or TZM-B1 cells. Mean \pm SD are shown; $n = 3-11$ mice used where indicated; Statistics (ns, $P > 0.05$; * $P < 0.05$; ** $P < 0.01$; *** $P < 0.001$): Log-rank (Mantel-Cox) test (**a, c, g** (left), **h** (left)), Unpaired *t* test (**b, d-f, g** (right), **h** (right), **i, k**), one-way ANOVA with Dunnett's analysis (**l, m, n**)

Therefore, CD4⁺ T cells would play profound roles in promotion of inflammatory leukocytosis and prevention of unleashed TLR4 inflammation of resident macrophages.

sCD4 is sufficient to hamper innate inflammatory response
The membrane CD4 molecule (mCD4) is conventionally reckoned as a co-receptor of TCR signaling in T cells. Intriguingly, the ectodomain of CD4 molecule (sCD4, D1-D4 domains) circulates in the blood of infectious and autoimmune diseases.³⁰⁻³² sCD4 in the serum steadily increased 24 h after mice received *i.p.* LPS (Fig. 3a), indicative of a compensatory anti-inflammation function. Indeed, incubation of recombinant sCD4 with BMDM prevented TLR4 inflammatory activation (Fig. 3b), with D1-D2 domains being sufficient (Fig. 3c). sCD4 had no apoptotic effect on macrophages (Supplementary Fig. 4a). Naïve T cells dampen a wide range of TLR-mediated inflammatory response in various innate immune cells.³ sCD4 could also effectively prevent TLR3 (polyI:C), TLR7 (VSV), or TLR9 (CpG ODN) activation of macrophages (Fig. 3d), and inhibited the inflammatory response of bone marrow-derived dendritic cells (BMDC) to LPS, as well (Supplementary Fig. 4b). SARS-CoV-2 Spike protein can directly target TLR4 to activate IL-1 β expression.³³ sCD4 protein effectively inhibited PICC response to SARS-CoV-2 infection of PBMC (Supplementary Fig. 4c). Critically, administration of sCD4 protein (200 μ g/mice) to WT mice 12 h before LPS injection protected mice from the lethal challenge (Fig. 3e), with a significant reduction of TNF/IL-6 (Fig. 3f). sCD4 also prevented CLP-induced hyperinflammation similarly (Supplementary Fig. 4d), by effectively inhibiting the activation of splenic resident macrophages (Supplementary Fig. 4e). sCD4 did not affect the numerical distribution of CD4⁺ or CD8⁺ T cells in the thymus and peripherals of LPS (Supplementary Fig. 4f) or CLP (Supplementary Fig. 4g) model. Impressively, administration of sCD4 (300 μ g/mice) 12 h before SARS-CoV-2 *i.n.* infection of K18-hACE2 mice attenuated the loss of body weight (Fig. 3g), reduced both PICC in the BALF (Fig. 3h) and pulmonary pathology (Fig. 3i). Therefore, CD4 molecule played a central role to control the homeostasis of TLR inflammatory responses of APCs, both in close contact (mCD4) and long range (sCD4).

CD4/MHCII engagement suppressed macrophage inflammation
MHC II is required for T cells to hamper innate inflammation.⁸ Specifically, MHC II transmitted the inhibitive signal of CD4 to TLR4 activation, because neither isolated CD4⁺ T cells (Fig. 4a) nor sCD4 (Fig. 4b) were able to prevent LPS activation of MHC II-deficient (MHC II^{-/-}) macrophages in vitro, or in MHC II^{-/-} mice (Fig. 4c, d). CD40L of CD4⁺ T cells can also downregulate macrophage TNF response to LPS through a paracrine activation of IL-10.³⁴ This process did not require MHC II, because trimeric CD40L protein (sCD40L) still inhibited TNF/IL-6 response to LPS in MHC II^{-/-} macrophages in vitro (Fig. 4e). On the other hand, sCD4 inhibited LPS inflammation as efficient in CD40L^{-/-} BMDM as in wt macrophages (Fig. 4f). Therefore, CD4 and CD40L of CD4⁺ T cells would function independently to prevent APC from TLR overactivation.

To critically test whether MHC II in macrophages per se is sufficient to mediate sCD4 antiphlogistic effect, macrophages were first depleted by clodronate liposome (Supplementary Fig. 5a). Macrophages depleted mice (Δ M Φ) partially resisted to lethal dose of LPS challenge (Fig. 4g), accompanied with reduced TNF/IL-6 (Fig. 4h). Consequently, sCD4 inhibited TLR4 inflammation only when MHC II^{+/+} (Fig. 4i), but not MHC II^{-/-} (Fig. 4j) macrophages were adoptively transferred to Δ M Φ mice. To further determine which subunit of MHC II was required to transmit the reverse signal of sCD4, different truncational mutants of MHC II subunits fused with eGFP were overexpressed in isolated peritoneal macrophages (Supplementary Fig. 5b for equal ectopic expression). Deletion of the cytoplasmic tails of MHCII A/E- α and A- β abrogated the inhibitive effect of sCD4 on TNF/IL-6 response (Fig. 4k). Therefore, these results suggested that MHC II in macrophages was sufficient to transmit CD4 reverse signal to suppress TLR hyperinflammation.

SHP2 was required to mediate MHC II crosstalk to TLR pathway
LPS is sensed by TLR4/MyD88, which recruits and phosphorylates IRAK1 to activate MAPK and NF- κ B signaling.³⁵ The previous results show that the cytoplasmic tail of MHC II can contact MyD88 to inhibit TLR4 signaling.³⁶ We then set to test whether sCD4 engagement of MHC II would take advantage of the same pathway to crosstalk to TLR pathway. Phosphorylation of IRAK1 in BMDM (Fig. 5a), as well as Erk, Jnk, p38 and I κ B α (Fig. 5b and Supplementary Fig. 6a), in response to LPS was effectively inhibited by sCD4. Importantly, sCD4/MHC II ligation antagonized specifically the TLR signaling, because TNFR mediated MAPK or NF- κ B activation was not affected (Fig. 5c). There are few reports that IRAK1 phosphorylation can trigger its proteosomal degradation, that may help reducing TLR4/NF- κ B activation.^{37,38} The total IRAK1 protein level slightly decreased even after a longer time of LPS stimulation (Fig. 5a, g). More experiments are needed to determine the role of IRAK1 degradation in MHCII reverse signaling.

Tyrosine phosphorylation plays an important role in the negative regulation of TLR signals.³⁹ The global tyrosine phosphorylation in LPS-treated BMDM was increased by sCD4 (Supplementary Fig. 6b), where SHP2 phosphorylation (Fig. 5d), but not Btk, Syk or SHP1 (Supplementary Fig. 6c), was specifically enhanced. SHP2 is a protein tyrosine phosphatase that regulates MyD88 signaling by contact with TRAF6.⁴⁰ LPS-induced binary interaction between SHP2 and TRAF6 was augmented by sCD4, as measured by reciprocal co-immunoprecipitation assays (Fig. 5e). Therefore, SHP2 would mediate CD4/MHC II crosstalk to TLR/MyD88 pro-inflammatory signaling. Indeed, sCD4 failed to inhibit TNF/IL-6 response to LPS in SHP2-deficient BMDM (Fig. 5f), where I κ B α (NF- κ B) and IRAK1 (MAPK) activation was restored (Fig. 5g). In mice with SHP2 specifically ablated in macrophages, sCD4 no long improved the survival rates of LPS sepsis (Fig. 5h), nor inhibited TNF/IL-6 response (Fig. 5i). Besides MyD88,³⁶ STING may associate with the membrane proximal/cytoplasmic domain of MHC II, probably through CD79, in APC cells.⁴¹ STING was also required for

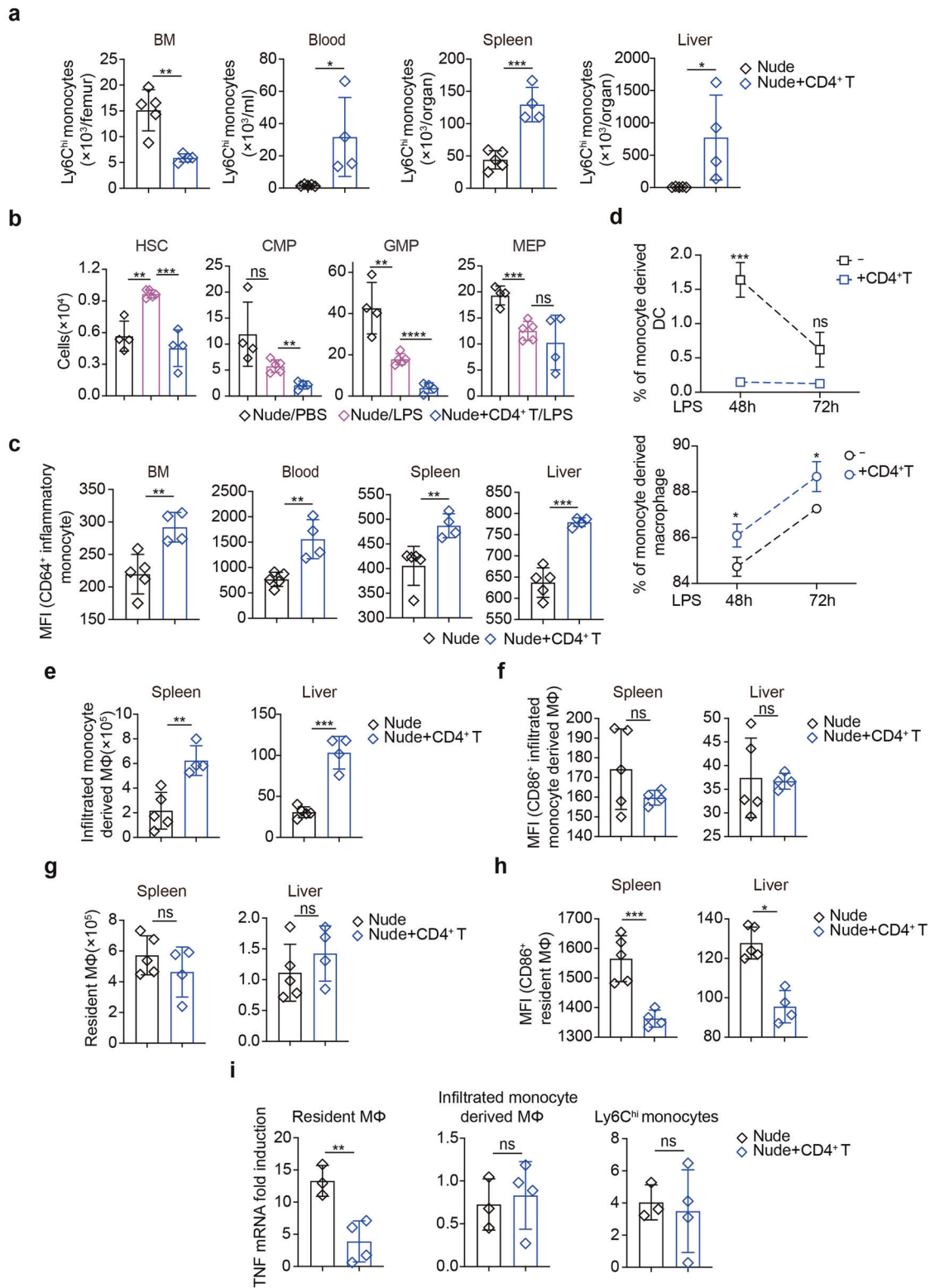


Fig. 2 CD4⁺ T promoted monocytes differentiation and dampened resident macrophage hyperinflammation. **a–c**, **e–i** Nude mice or nude mice reconstituted with CD4⁺ T cells were treated *i.p.* LPS for 3 h before indicated analysis. Cell numbers of **(a)** Ly6C^{hi} monocytes, **(b)** progenitor cells in BM (HSC, GMP, CMP, MEP), and **(c)** activated monocytes (CD64⁺) in the indicated organs were flow cytometric analyzed. **d** Proportions of indicated cell types after *in vitro* differentiation of BM-derived monocytes co-cultured with CD4⁺ T cells, for the indicated time of LPS treatment. Cell numbers of **(e)** infiltrated monocyte derived macrophages or **(g)** resident macrophages and **(f, h)** their activation status (CD86⁺). **i** TNF mRNA induction by LPS in the indicated cell types sorted from the spleen. Mean ± SD are shown; *n* = 3–5 mice used where indicated; Statistics (ns, *P* > 0.05; **P* < 0.05; ***P* < 0.01; *****P* < 0.001): Unpaired *t* test

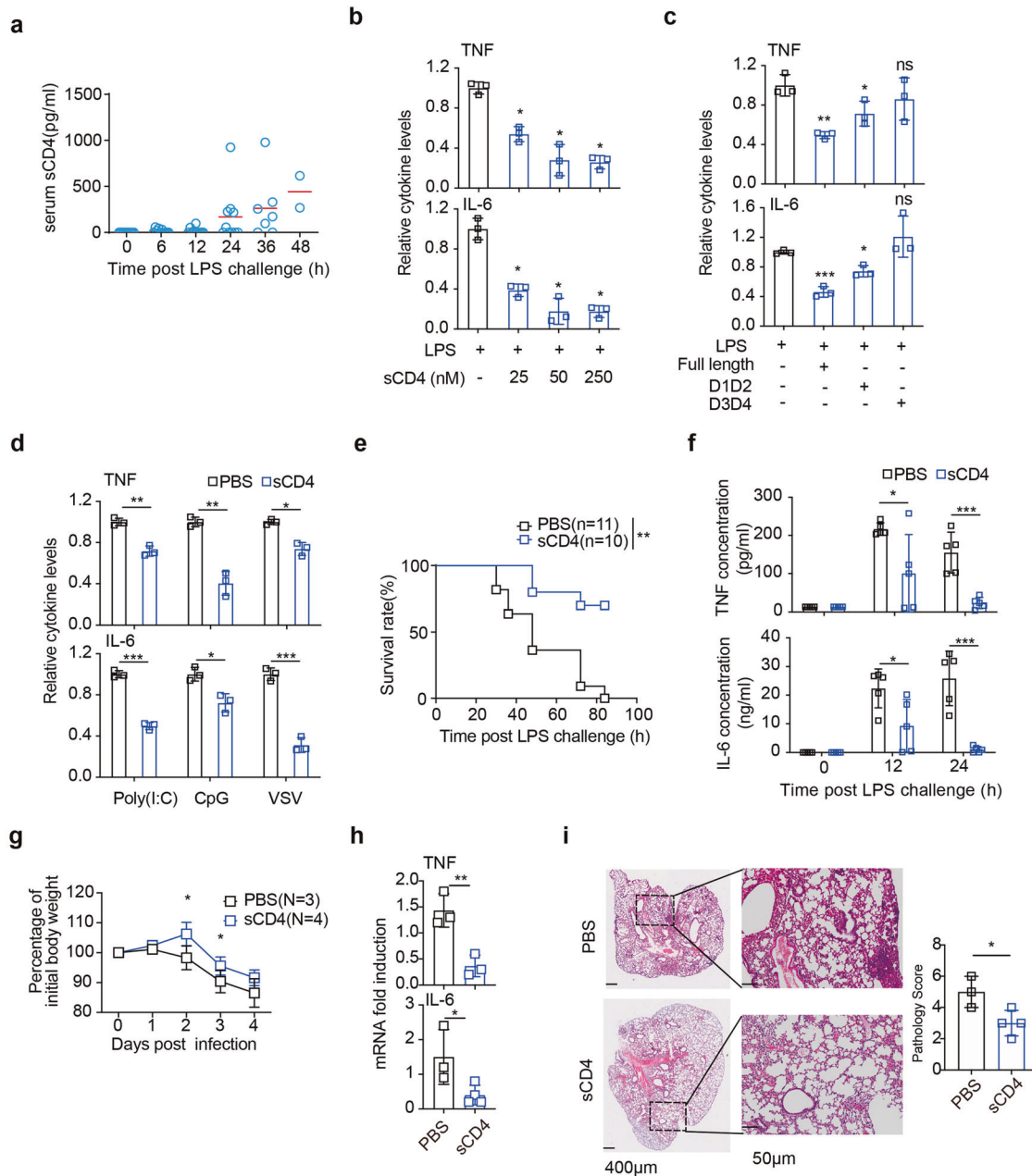


Fig. 3 sCD4 protein effectively dampened TLRs inflammation. **a** ELISA measurement serum sCD4 after mice ($n = 10$) received LPS for the indicated time. TNF/IL-6 production 16 h after LPS stimulation of BMDM pre-incubated with 50 nM of **(b)** sCD4, **(c)** different ectodomains of sCD4, or **(d)** sCD4 but LPS was replaced with agonists for poly(I:C) (100 $\mu\text{g}/\text{mL}$), CpG-ODN (0.03 μM) or VSV (MOI = 5). **e** Survival rates and **(f)** serum TNF and IL-6 levels at the indicated time after WT mice were injected with sCD4 (10 mg/kg) ($n = 10$) or PBS ($n = 11$), 12 h before LPS challenge. **g–i** Changes of body weights after hACE2 mice pre-treated with sCD4 were infected with SARS-CoV-2 for 4 days **(g)**. **h** TNF and IL-6 mRNA in lung by qPCR and **(i)** representative sections and pathology score of the lobe of left lung (with respective magnifications of areas of interest) on day 4. Mean \pm SD are shown; $n = 3–5$ mice used where indicated; Statistics (ns, $p > 0.05$; * $P < 0.05$; ** $P < 0.01$; *** $P < 0.001$): Log-rank (Mantel-Cox) test **(e)**, Unpaired t test **(d, f, g–i)**, one-way ANOVA with Dunnett’s analysis **(b, c)**

CD4/MHC II reverse signaling, since sCD4 no longer improved the survival rates of LPS sepsis (Fig. 5j), nor inhibited TLR4 inflammation in either STING^{-/-} mice (Fig. 5k) or STING^{-/-} macrophages in vitro (Fig. 5l). Together, these results suggested that SHP2 and STING might bridge CD4/MHC II inhibitory crosstalk to TLR4/MyD88 pro-inflammatory signaling.

sCD4 engagement dissociated the membrane raft domain of MHC II and TLR4

Because the cytoplasmic tail of MHC II is short and devoid of ITIM or ITAM motif, it was critical to test whether and how STING and/

or SHP2 directly tethered to MHC II. Duolink proximity ligation assays (PLA) were performed to measure these potential intermolecular interactions (Fig. 6a, red dots). At the resting state of cultured BMDM, SHP2 and STING, including activated SHP2 (pY580), were associated with MHC II. The interactions between MHC II and TLR4 in the cytoplasmic membrane, and MHC II with STING oligomerized in ER/Golgi⁴² activated by LPS, were effectively disrupted by sCD4 (Fig. 6a). LPS dissociated the activated SHP-2 with MHC II, which could be effectively reverted by sCD4 (Fig. 6a). Merge of fluorescent antibody labeled MHC II (red) with Duolink dots of SHP2/STING (green) showed that SHP-2

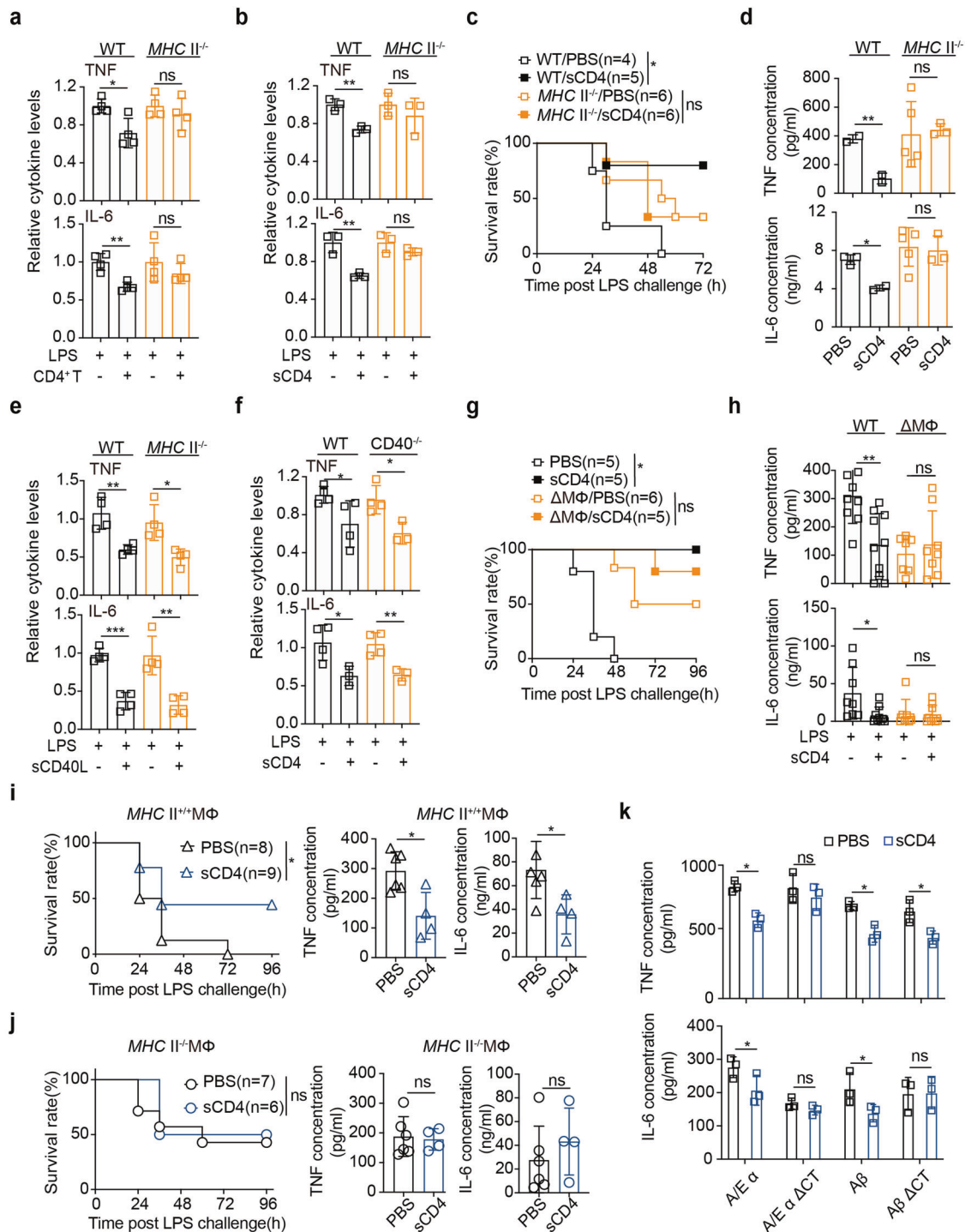


Fig. 4 sCD4 downregulated TLR4 inflammation through MHC II in macrophages. **a, b** TNF/IL-6 measurement as in Fig. 11 except that *MHC II^{-/-}* BMDM were co-cultured with **(a)** an equal number of CD4⁺ T cells, or **(b)** 25 nM sCD4 protein. **c** Survival rates and **(d)** serum TNF/IL-6 24 h after LPS *i.p.* injection in wt littermates or *MHC II^{-/-}* mice pre-treated with a single dose of sCD4 (10 mg/kg). TNF/IL-6 in supernatants after **(e)** *MHC II^{-/-}* BMDM were pre-treated with 25 nM sCD40L, or **(f)** *CD40^{-/-}* BMDM cells with 25 nM sCD4 before LPS stimulation. Survival rates and serum TNF/IL-6 in mice with **(g-h)** macrophages ablated ($\Delta M\Phi$) or **(i-j)** $\Delta M\Phi$ mice reconstituted with either *MHCII^{+/+}* or *MHCII^{-/-}* macrophages, that received 10 mg/kg sCD4 or PBS before *i.p.* LPS stimulation. **k** TNF/IL-6 in the supernatants 12 h after peritoneal macrophages that transiently overexpressed with the indicated MHCII subunits or cytoplasmic tail-truncational mutants (ΔCT) were stimulated with LPS or LPS plus 25 nM sCD4. Mean \pm SD are shown; $n = 3-10$ mice used where indicated; Statistics (ns, $P > 0.05$; * $P < 0.05$; ** $P < 0.01$; *** $P < 0.001$): Log-rank (Mantel-Cox) test (**c, g, i** (left), **j** (left)), Unpaired *t* test (**a-b, d, e-f, h, i** (right), **j** (right), **k**)

and STING could form complex and were in close proximity to MHC II, and sCD4 reduced the assembly of MHCII-SHP2/STING complex (Fig. 6b). Furthermore, sCD4-increased pSHP-2/MHC II interaction was abolished in *TLR4^{-/-}* BMDM (Supplementary Fig. 7a),

suggesting that SHP-2, probably through complexing with STING, function to couple MHCII-TLR4 crosstalk for sCD4. These results would suggest that sCD4 dissociated LPS/TLR4 from MHC II/STING complex with presumably assistance of the activated SHP2.

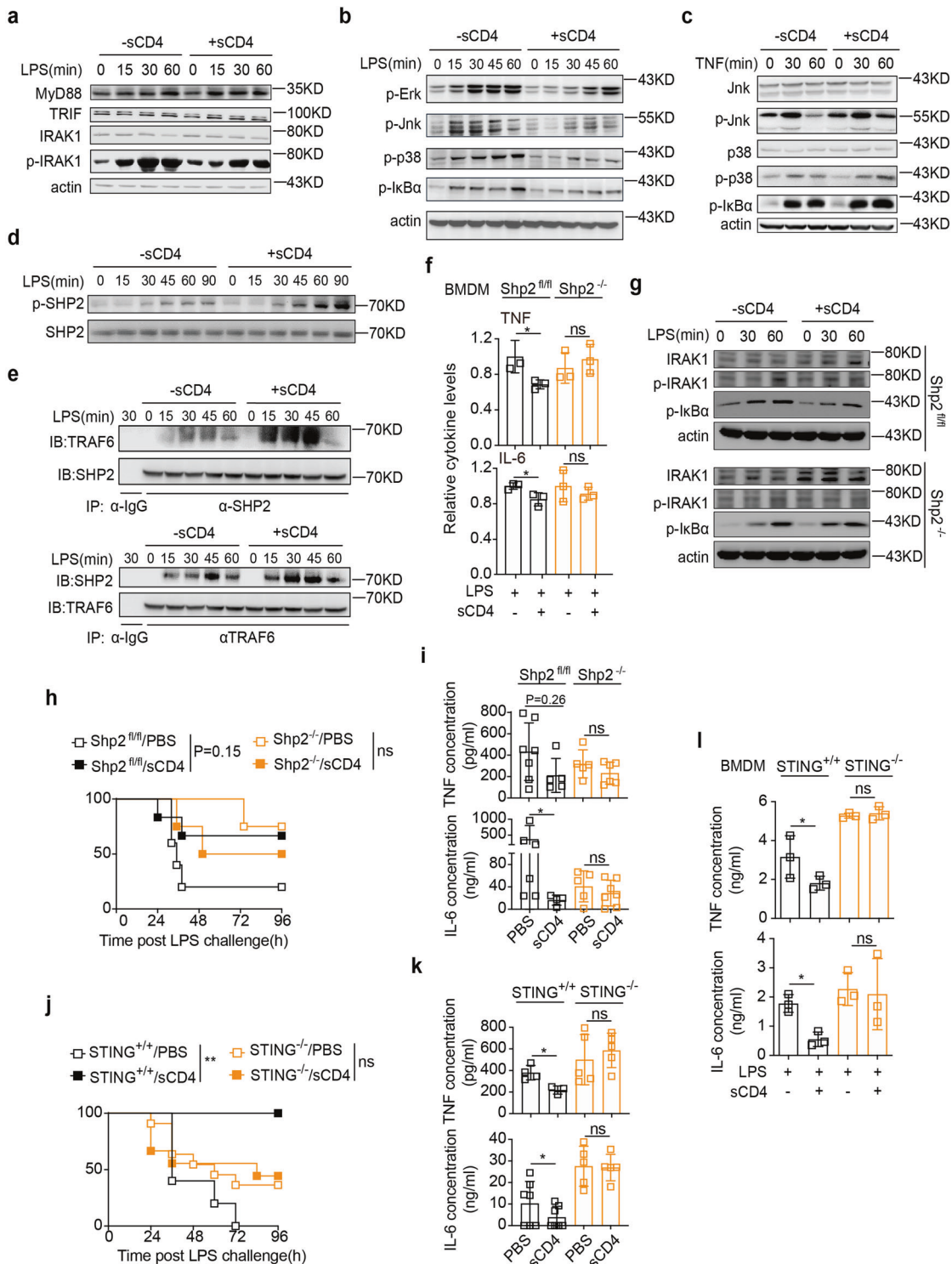


Fig. 5 SHP2 and STING mediated CD4/MHC II crosstalk to TLR signaling. BMDM cells were incubated with (a–b, d–e) 100 ng/mL LPS or (c) 5 ng/mL TNF in the presence or absence of 25 nM sCD4 for the indicated time. a–d Western blotting of the indicated proteins. e Reciprocal co-immunoprecipitation between SHP2 and TRAF6 in pm cells. f TNF/IL-6 in supernatants were measured as in Fig. 3B except for that SHP2^{-/-} BMDM used. g Western blots as in panels (a–b) except that SHP2^{-/-} BMDM were used. SHP2^{fl/fl} macrophages were used as controls. h Survival rates and (i) serum TNF/IL-6 were measured at the indicated time after *i.p.* LPS in macrophage specific SHP2^{-/-} mice that received sCD4 (10 mg/kg). j Survival rates and (k) serum TNF/IL-6 levels 12 h post LPS injection of STING^{-/-} mice. l TNF/IL-6 in supernatants 4 h after LPS treatment of BMDM isolated from STING^{-/-} or wt mice in the absence or presence of sCD4 (25 nM). Mean ± SD are shown; $n = 3–6$ mice used where indicated; Statistics (ns, $P > 0.05$; * $P < 0.05$): Unpaired *t* test (f, i, k, l), Log-rank (Mantel-Cox) test (h, j)

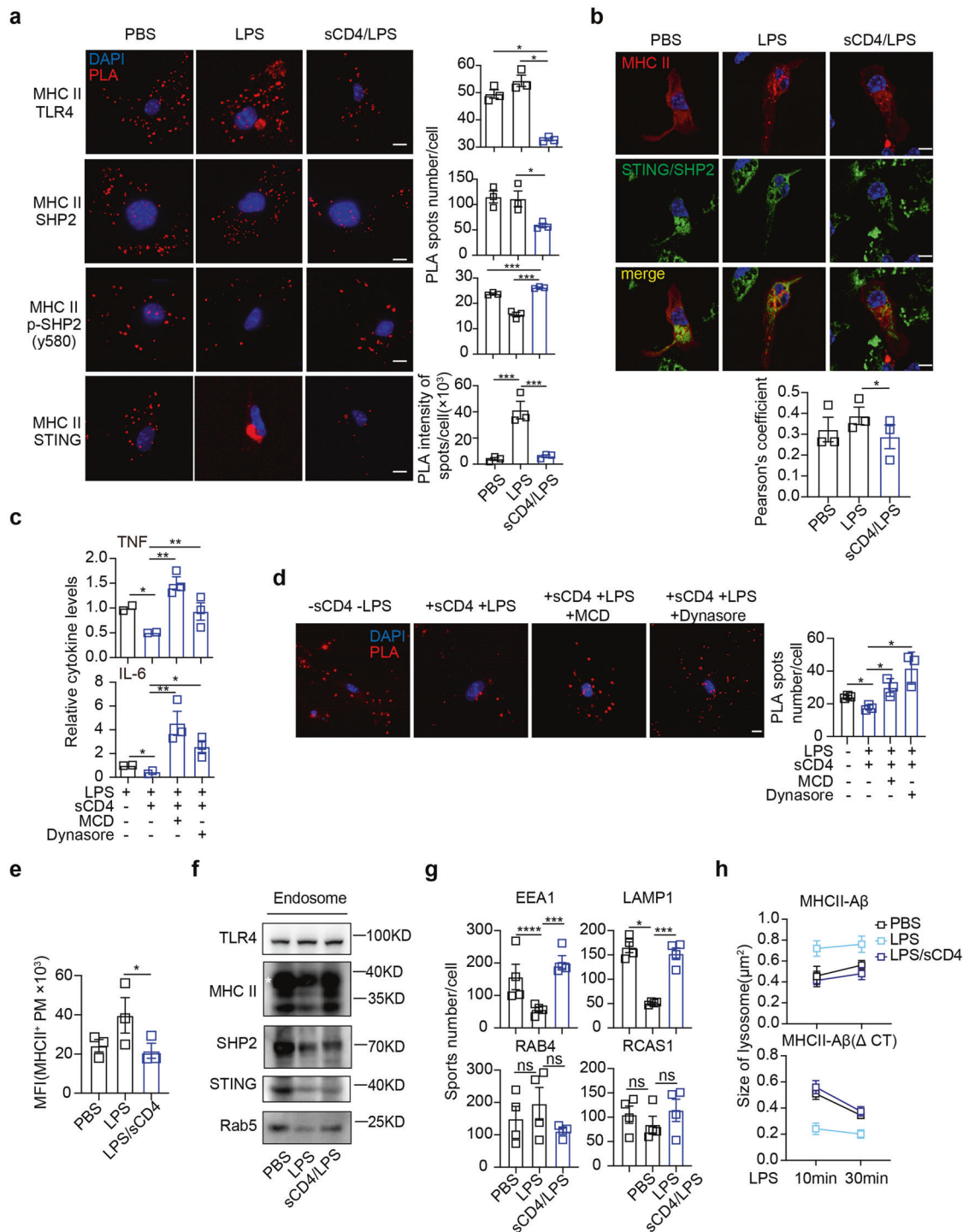


Fig. 6 sCD4 disrupted MHCII/TLR4 rafts and reduced LPS/TLR4 inflammatory membrane confinement. Duolink assays to quantify protein-protein interactions of (a) the indicated pairs (red), or (b) between STING and SHP2 (green) that combined with immunofluorescent staining of MHC II (red) in BMDM. Tripartite colocalization indicated in yellow. The nuclei counter-stained with DAPI. Pearson's coefficients indicated the degree of colocalization. Bar = 5 μm. c TNF and IL-6 in supernatants 30 min after peritoneal macrophages treated with LPS or LPS plus sCD4, in the presence of indicated endocytosis inhibitors. The average of two independent repeats. Three replicate wells were used for each condition where the indicated inhibitor was added. d Duolink spots of MHC II-SHP2 interactions and (e) flow cytometric analyses of cell surface MHC II. Bar = 5 μm. Macrophages (5 × 10⁶) were treated with LPS/sCD4 for 1 h, and (f) endosomes were isolated for immunoblot analysis of the indicated proteins (asterisk), or (g) organelle numbers per cell were quantified after immunofluorescence staining of EEA1 (early endosomes), LAMP1 (lysosomes), RAB4 (recycling endosome) and RCAS1 (Golgi). h Lysosomes size was quantified using LysoTracker after RAW264.7 cells were transfected with GFP-tagged MHC II Aβ or MHC II AβΔCT. Several view fields were randomly selected and images were acquired every 10 s for 20 min of LPS or LPS plus sCD4 treatment. Mean ± SD are shown; n = 3–4 mice used where indicated; Statistics (ns, P > 0.05; *P < 0.05; **P < 0.01; ***P < 0.001); Unpaired t test

LPS confines TLR4 in membrane rafts so as to transmit pro-inflammatory signaling.^{30,43} Inhibitors of lipid raft- (MCD) or clathrin- (Dynasore) mediated endocytosis impaired the ability of sCD4 to antagonize TLR4 inflammation (Fig. 6c) or dissociate SHP2 from MHC II (Fig. 6d). Therefore, the pro-inflammatory LPS/TLR4 raft compartments might be disrupted by sCD4 engagement of MHCII membrane domains. On the other hand, sCD4 abrogated MHC II upregulation in BMDM surface by LPS, both by fluorescence staining (Fig. 6e and Supplementary Fig. 7b) and and flow cytometry detection (Supplementary Fig. 7c), suggesting that sCD4 engagement might augment MHC II internalization^{44–46} and/or lysosomal targeting.⁴⁶ LPS reduced overall the formation of early endosomes (Rab5), and concomitant endosomal distribution of MHC II, SHP2 and STING. sCD4 treatment, however, significantly restored their endosome trafficking (Fig. 6f). In addition to increased early endosome formation (EEA1), sCD4 also accelerated LAMP1-stained lysosome formation (Fig. 6g and Supplementary Fig. 7d) of MHC II complex. Live cell imaging indicated that sCD4-driven endosome-lysosome fusion relied on the cytoplasmic domain of MHC II- $\alpha\beta$ (Fig. 6h), in agreement with the previous finding that MHC II cytoplasmic domain controls its endocytotic presentation.⁴⁷ Therefore, these results suggested that sCD4 disrupted pro-inflammation raft domains of MHC II/TLR4 complex, and by augmenting MHC II endocytosis, to destabilize pro-inflammatory membrane confinement of TLR4.

DISCUSSION

T lymphopenia occurs in the early phase of septic hyperinflammation,¹⁶ is commonly associated with morbidity and mortality of septic infections.¹⁷ Whether and how such a stoichiometric control of innate hyperinflammation is rooted in numerical reduction of naive CD4⁺ T cells, or CD4 molecule per se, remains elusive. This work establishes unambiguously that systemic hyperinflammation upon infection was aggravated by the loss of CD4⁺ T cells, that unleashed the restrains of MHC II/TLR4 inflammatory "signalosome" for cytokine storm or cytokine release syndrome in sepsis. This conclusion does not intend to exclude the contribution of CD8⁺ T lymphopenia in sepsis also observed in LPS and CLP models. Previous report showed that CD8⁺ T cells are able to engage MHC I to inhibit TLR inflammation.⁴⁰

CD4 molecule has been extensively studied, both structurally and functionally, as a co-receptor of TCR in facilitating MHC II-restricted T-cell recognition.⁴⁸ CD4 contacts a conserved membrane-proximal region of MHC II, an action independent of TCR.⁴⁹ It has long been established that CD4/TCR complex uses MHC II as a receptor to feedforward activate antigen presentation signaling.⁵⁰ However, whether and how CD4/MHC II engagement negatively regulates APC inflammatory response to invading pathogens has never been addressed before. We revealed in this work that, CD4 molecule may function as an inhibitory ligand of MHC II, independent of TCR or CD40L, to constrain TLR inflammatory activation of resident macrophages, rather than monocyte-derived macrophages that had infiltrated to the lesion. CD4/MHC II engagement to downregulate TLR inflammation did not involve APC apoptosis, apparently different from the actions of antibodies or cognate TCR engagement of MHC II that accelerate cell death of activated DC,^{51,52} macrophages^{53,54} and B cells,^{55,56} in caspase-independent, PKC/ERK-dependent manner. This and the previous work^{3,57} also showed that TCR engagement is not essential for naive CD4⁺ T cells to inhibit PICC response in APC. Of course, CD4⁺ T cells may utilize co-inhibitory molecules, BTLA⁵⁸ or CD40L³⁴ to down-regulate TNF response to LPS. CD40L signaling in effector/memory CD4⁺ T cells, independent of TCR, inhibits IL-1 β secretion by APCs.¹⁰ Other TNF superfamily members, RANKL, LIGHT, 41BBL, CD30L and OX40L, may also be involved in such an inhibitory T-APC immunological synapse. This work further show that CD4 molecule functions independent of

CD40L, and not involving TNFR signaling, that essentially regulates the homeostatic APC inflammatory response.

Previous studies using antibody cross-linking,⁵⁹ super antigens^{60,61} or lymphocyte-activating gene-3 (LAG-3), a MHC II ligand,⁶² demonstrate that the heterodimeric MHC II protein complex can function as a receptor to activate T-dependent B cell response. In this context, an array of trans-membrane proteins, including CD79, CD19, CD20, CD21, CD40 and among others, physically associate with MHC II for B cell activation and differentiation.⁵⁰ Intriguing enough, we showed additionally that SHP2 activation and association with MHC II cytoplasmic tail, but not SHP1, was required for CD4 inhibition of TLR4/MyD88 signaling and IRAK1/Erk activation. STING/SHP2 interaction has been shown in cytosolic DNA activated JAK1/STAT1 signaling.⁶³ This is in line with previous observations that STING promotes MHC II-aggregation induced B lymphoma cell death and Erk activation independent of SHP1,⁶⁴ albeit SHP1 can associate with STING.⁶⁵ SHP2 also inhibits TLR3/TRIF signaling pathway in human monocytes.⁶⁶ It remains to test whether CD4 inhibition of TLR3 inflammation requires SHP2. Furthermore, sCD4/MHC II engagement did not alter LPS-induced phosphorylation of Btk, different from intracellular MHC II, which can interact and activate Btk via CD40 to promote endosomal TLR signaling.⁶⁷ Therefore, it is tempting to speculate that cell surface and intracellular MHC II may use different mediators to sort TLR signaling.

Importantly, we showed that increased serum sCD4 associated with LPS hyperinflammation. sCD4, presumably shed by a MMP-like sheddase, is also increased in patients of chronic inflammatory diseases, and correlates positively with the disease activities and poor prognosis in RA patients.⁶⁸ This would emphasize a compensatory effect of the increased sCD4 in control of inflammation, albeit sCD4 at sub-nanomolar concentrations in these patients is insufficient to do so. The binding affinity of CD4 ectodomain to pMHC II (~150–200 μ M) is relatively weak as measured in vitro.⁶⁹ This far exceeds the concentrations of sCD4 needed for 50% inhibition of TLR4 hyperinflammation in vitro (~25 nM) or in vivo (~125 nM). We reason that auxiliary factors assembled within MHC II/TLR compartments in macrophages might help offset the low affinity of CD4 to MHC II. The exact makeup and function of MHC II/TLR rafts targeted by CD4 in this context remain to be determined. At least, TNFR is not associated with MHC II/TLR 'signalosome'. A nanomolar IC₅₀ would potentially make sCD4 (~10–15 mg/kg) especially desirable to prevent the onset of fatal sepsis. This work thus indicated that sCD4 might provide a new antiphlogistic paradigm to prevent severe/critical SIRS or sepsis. Applying sCD4 protein to target inflamed innate cells is apparently advantageous over the current therapeutics,⁷⁰ e.g., corticosteroid or antibodies, that target PICC or their cognate receptors (Supplementary Fig. 9).

MATERIALS AND METHODS

Mice

Mice homozygous null for MHC II genes (B6.129S-H2^{dlAb1-Ea}/J) were kindly provided by Dr. Xue-tao Cao (National Key Laboratory of Medical Immunology, Naval University of Medicine, Shanghai, China), SHP-2^{fl/fl} and LysM-cre knock-in mice by Drs. Hui Xiao and Gen-Sheng Feng, STING^{-/-} mice by Dr. Xin-wen Chen (Wuhan Institute of Virology, Chinese Academy of Sciences). K18-hACE mice (C57BL/6 background) were purchased from Gem Pharmatech (Jiangsu, China). CD40-deficient mice were generated by CRISPR-Cas9 approach. Guide RNA sequences were listed in Supplementary Table 2. Littermates of 6–8 weeks (body weight and gender matched) were used, unless otherwise mentioned. Where used, nude mice, BALB/c and C57BL/6J mice were from Vital River Lab Animal Tech (Beijing). All mice were bred under specific pathogen-free conditions, founder mice and breeding

littermates were genotyped by PCR (primers in Supplementary Table 3, and results in Supplementary Fig. 8). All animal experiments were performed in accordance with institutional guidelines and were approved by the Animal Care and Use Committees of the Institute of Biophysics or Institut Pasteur of Shanghai, Chinese Academy of Sciences (No. A2020043).

Reagents and antibodies

LPS (0111:B4), CpG ODN and poly (I:C) were purchased from Sigma-Aldrich (St Louis, USA). Mouse recombinant CD4 (His-tag), CD40L (Fc-tag) and TNF (Fc-tag) proteins were from Sino Biological. D1-D2 (Fc- or 6xHis-tag) and D3-D4 (His-tag) of CD4 were generated by Bac-to-Bac Baculovirus Expression System (FulGen). LysoTracker Deep Red was from Life Technologies. Antibodies against indicated proteins used in this study were: CD4 (GK1.5 and RM4-5) from eBioscience, mouse IgG2a isotype control antibody (401501) and MHC class II (107610) from BioLegend; TRIF (ab13810), β -actin, Goat anti-Rat Alexa Fluor 647(A-21247), Donkey anti-Mouse IgG Alexa Fluor 488(A-21202) and Goat anti-Rabbit Alexa Fluor 555(A-21429) from Thermo Fisher; TRAF6 (sc-8409) from Santa Cruz; MyD88 (D80F5), IRF3 (D83B9), Syk (D3Z1E), Btk (D3H5), IRAK1 (D51G7), Erk (9102), IgG (7074, 7076), Jnk (56G8), p38 (9212), SHP-2 (D50F2), phospho-Erk at Thr202-Tyr204 (E10), phospho-Jnk at Thr183-Tyr185 (G9), phospho-SHP-2 at Tyr580 (5431), phospho-p38 at Thr180-Tyr182 (9211), phospho-IRF3 at Ser396 (4D4G), phospho-IkBa at Ser32-Ser36 (5A5), phospho-Btk at Tyr223(D9T6H), phospho-Syk at (Tyr352), phospho-Tyrosine antibody (p-Tyr-100), EEAL (C45B10), LAPM1 (D2D11), RAB4 (2167T) and RCAS1(D2B6N) from Cell Signaling Technology; RAB5(AR038) from Beyotime. SHP1 (ab32559), SHP-2 (ab131541), phospho-SHP1 at Y536 (ab51171), anti-MHCII (ab180779), anti-MHCII (ab25681), anti-TLR4 (ab22048), anti-SHP2 (ab131541), anti-P-SHP2 (ab62322) mouse IgG isotype control (ab172730), rabbit IgG isotype control (ab37355) from Abcam; STING (66680-1-Ig) from Proteintech. Phospho-IRAK1 at T209 (ab218130) from Sigma-Aldrich.

Mouse models of sepsis

The endotoxemia mouse model was established by *i.p.* injection of LPS (8–10 mg/kg body weight) in either C57BL/6J or nude mice. Where indicated, mice were *i.p.* injected with sCD4 (10 mg/kg) 12 h before LPS *i.p.* injection or transferred with CD4⁺ T cells 7 days before LPS injection. The cecal ligation and puncture (CLP) induced polymicrobial sepsis were performed as previously described.⁷¹ Briefly, the mice were anesthetized, and a small midline abdominal incision was made. The cecum was then exteriorized, and the distal three-quarters of the cecum was immediately ligated without causing intestinal obstruction. The ligated cecum was punctured with an 18-gauge needle, and a small amount of feces was gently squeezed out of the perforation to ensure patency of the punctures. The cecum was then relocated into the abdominal cavity, and the incision was closed. In the sham surgical controls, the cecum was exposed without ligation or puncture. At the indicated time points, mice were euthanized and the intestine, thymus, liver, spleen, and peripheral blood were collected for analysis. Thymus were fixed in 4% PFA solution and for histological stainings.

Histology

Left lobes of lung or thymus were fixed in 4% paraformaldehyde and embedded in paraffin. Fixed tissues were sliced into 5 μ m thick sections and stained with hematoxylin and eosin (H&E). To obtain a whole slide image, the slides with Mount coverslip onto the section on glass slide with neutral resins and subsequently the imaging data were obtained with Vectra3 with 20 \times objective (PerkinElmer, Vectra 3). Degrees of pathological alteration were scored following the standards described in Supplementary Table 4.

CD4⁺ T cell depletion and adoptive transfer

CD4⁺ T cell depletion was performed as previously described using CD4 antibody (200 μ g in 250 μ L GK1.5, *i.p.*) or isotype antibody every 3 days. Splenic CD4⁺ T cells were enriched with mouse CD4⁺ T cell negative isolation kit (Easy SepTM, >95% purity, Stemcell, Canada) and *i.p.* transferred to recipient mice (2 \times 10⁶ cells/mouse) for 7 days.

Salmonella typhimurium infection

Salmonella typhimurium (strain SL1344) was grown overnight at 37 $^{\circ}$ C and then subcultured the next day in fresh LB to OD₆₀₀ = 0.6–0.8 at 37 $^{\circ}$ C. Water and food were withdrawn 4 h before gavage, mice (C57/B6j, male, 8 weeks old) were inoculated with 1 \times 10⁸ bacteria by oral gavage. Drinking water and food were supplied immediately. After 60 h, mice were euthanized and the blood, and spleen were harvested for bacterial loads, cytokines and immune cells analyses.

COVID-19 patients

Study approval. This study was approved by the Research Ethics Committee of Shenzhen Third People's Hospital, China (approval number: 2020-181) and the written informed consents were obtained from enrolled patients.

Patients and samples. The study enrolled 15 patients (male:female = 13:2; ages 36 to 73) diagnosed positive for SARS-CoV-2 infection in January 2020 (Supplementary Table 1, qPCR, nasopharyngeal swab and throat swab specimens), and negative for influenza A/B, RSV or adenovirus co-infection. Chest computed tomographic scans showed varying degrees of bilateral lung patchy shadows or opacity. Their clinical manifestations were determined as according to the Diagnosis and Treatment Protocol of COVID-19 (the 7th Tentative Version) by National Health Commission of China issued on March 3, 2020. Severe patients were diagnosed based on one of the following criteria: (1) Respiratory distress: RR \geq 30 times/min; (2) Fingertip oxygen saturation \leq 93% at resting state; (3) Arterial partial pressure of oxygen (PaO₂)/fraction of inspiration oxygen (FiO₂), P/F \leq 300 mmHg (1 mmHg = 0.133 kPa); (4) Patients with obvious progress of lesions in 24–48 h shown by pulmonary imaging >50%.

All patients were hospitalized at Shenzhen Third People's Hospital 1 to 16 d after symptom onset. Among these patients, 11 had exposure history after traveling to Wuhan and other 4 had direct contact with COVID-19 patients from Wuhan. All patients presented with fever, fatigue and dry cough, and 5 had developed severe pneumonia when admitted to the hospital (patient number C3, C4, C8, C11, C14). Eleven patients had underlying disease such as hypertension, cardiopathy, autoimmune disorder or chronic hepatitis B. All patients progressed from mild to severe pneumonia, or severe to mild pneumonia, and all recovered and discharged after symptomatic treatment. Patient C11 succumbed to COVID-19 in hospital. All patients received interferon and ribavirin and lopinavir and/or methylprednisolone treatments.

Isolation of BALF and PBMC. BALF samples were obtained and placed on ice, passed through a 100 μ m nylon cell strainer to remove clumps and debris, centrifuged (1000 \times g, 10 min). Supernatants (25 μ L) were mixed with equal volume of sonication beads and detection antibodies for IL-1 β , IL-2, IL-4, IL-5, IL-6, IL-8, IL-10, IL-12p70, IL-17, IFN- α , IFN- γ or TNF- α (Uni-medica, Shenzhen, China) on a shaker (500 rpm, room temperature, 2 h). SA-PE (25 μ L) was added directly to each tube and mixed for 30 min before flow cytometric analysis (Canto II, BD). Data were analyzed using LEGENDplex v8.0 software (VigeneTech Inc.). Anticoagulant blood was used to measure CD3⁺CD4⁺ and CD3⁺CD8⁺ T cell counts by flow cytometry. All procedures were performed within 2 h after specimen collection in a BSL-3 laboratory approved by Ethics

Committees of Shenzhen Third People's Hospital (SYB3-2020003). PBMC was isolated from blood samples using standardized density gradient technique (Ficoll-Paque).

SARS-CoV-2 infection of PBMC

PBMC (5×10^5 cells/ml) were seeded in 96-well plate with RPMI-1640 for 12 h before incubation with 50 nM sCD4 for additional 2 h. Cells were then infected with SARS-CoV2 (separated from patient YCJ. MOI = 0.1 or 0.5, respectively). Supernatants were collected after 24 h of infection, and the virus was inactivated using β -lactone (Solarbio) at 4 °C for 36 h. TNF and IL-6 were measured by using Elisa kit (BioLegend). Experiment performed in a Bio-safety Level 3 facility.

SARS-CoV-2 infection of hACE2 transgenic mice

Mice were used following institutional ethics guidelines and approved by the Animal Care Committee of Naval Medical University (No.# NMUP3LP20201109-2). K18-hACE2 transgenic C57BL/6 mice (male, 10 weeks old) were *i.p.* injected 500 μ g of GK1.5 antibody (in 200 μ L PBS) to deplete CD4⁺ T cells 24 h before infection. For sCD4 treatment, 300 μ g of sCD4 (in 200 μ L PBS) was *i.p.* administered 12 h before infection. SARS-CoV-2 virus (pfu 1×10^2 in a final volume of 50 μ L PBS) was *i.n.* infected. Mice were then euthanized at 7 d post infection (CD4⁺ T cell depletion group) or 4 d (sCD4 pre-treatment group), and lungs were harvested for indicated analyses.

Plasmid construction and transfection

MHC II A/E α (NM_010378.3) and A β (NM_207105.3) cDNA were subcloned into vector pEGFP-N1. The cytoplasmic domain of MHC II was replaced with 3 x Gly (designated as MHCII A/E α Δ CT and A β Δ CT). For transient expression of the indicated MHC II chains, the plasmids were electroporated to peritoneal macrophages using the Neon Transfection System (ThermoFisher). Typically, 1×10^6 cells were transfected with 1 μ g plasmid (1200v, 30 ms; twice).

Flow cytometry

DN T cells, monocytes and macrophages in the spleen, or DN T and SP CD4⁺ T cells in the thymus were isolated (1×10^7 splenocytes/thymocytes labeled with 5 μ g indicated antibodies in 1 mL staining buffer (PBS, 1% FBS)) by FACSAria II sorter (BD Biosciences). Multicolor flow cytometric analyses were routinely performed on LSR Fortessa (BD Bioscience) and analyzed by FlowJO software (Tree Star, OR). Dead cells were excluded with 7-AAD (eBioscience) or DAPI (BD Biosciences). Detailed antibodies information in Supplementary Table 5. Analysis of apoptosis was performed with Annexin V-FITC Apoptosis Detection Kit according to the manufacturer's instruction (BD Biosciences).

Co-culture and PICC measurements

Bone marrow cells were isolated from 6–8 week old C57BL/6 mice. After red blood cells were lysed with RBC lysis buffer (eBioscience), cells were seeded in RPMI-1640 medium containing 10% FBS (Gibco) and 1% Pen-Strep. M-CSF (20 ng/mL, PeproTech), or GM-CSF (20 ng/mL) and IL-4 (10 ng/mL, PeproTech), were used for BMDM or BMDC differentiation, respectively. BMDM and BMDC were used on days 7–8, with fresh media containing cytokines replaced every 2 days. CD4⁺ T cells (5×10^4) were co-cultured 1:1 with differentiated BMDMs or BMDCs for 2 h. Where indicated, 25 nM sCD4 or sCD40L protein (Sino Biological) was added to the culture overnight. BMDM or BMDC cells were seeded in a 96-well plate and stimulated with 100 ng/mL LPS, 100 μ g/mL poly(I:C), 0.3 μ M CpG ODN or VSV (MOI = 5) for 16 h, before the supernatants were collected for cytokine measurements by Luminex analyses using the Procartaplex Mouse 2-plex kit (eBioscience), Mouse 26-plex kit (Thermo Fisher) or Human 11-plex kit (eBioscience). The concentration of cytokines were detected and analyzed by Bio-Plex 200 System (Bio-Rad).

ELISA analysis of serum sCD4

To measure mouse CD4 in sera, 96-well high binding plates (NEST) were coated with anti-CD4 (GK1.5, BioLegend), followed by an incubation with 10 μ L two-fold serially diluted samples to be tested. After washing, the wells were incubated with biotinylated anti-CD4 (RM4-4, BioLegend) and subsequently with HRP-coupled streptavidin. The levels of sCD4 were photometrically determined according to the manufacturer's manual (Sino Biological). The results are presented as mean \pm SEM of at least three samples.

Quantitative real-time PCR

Total RNA was extracted with RNA extraction kit (R4012-02, Magen, CN) according to the manufacturer's instructions. Quantitative real-time PCR(qPCR) was performed with ABI QuantStudio 1 (ThermoFisher) using SYBR RT-PCR kit (Bio-Rad). The primers used in this study were: tnf forward primer 5'-TCTTCTCCTCCTGATCGTG and reverse primer 5'-GAAG ATGATCT GACTGCCTG; il-6 forward primer 5'-TACCCCCAGGAGAAGATT CC and reverse primer 5'-TT TTCTGCCAGTGCCTCTTT. gapdh forward primer 5'-TGCACCACCAA CTGCTTAGC and reverse primer 5'-GGCATGGACTGTGGTCATGAG. Results were normalized to *gapdh* mRNA levels.

Immunoblot and immunoprecipitation

Where indicated, membrane proteins were extracted using Minute Plasma Membrane Protein Isolation and Cell Fractionation Kit (SM-005; Invent). Whole cell lysates were routinely prepared as previously described,⁷² and protease inhibitors cocktail (Roche) added before immunoprecipitation. Total protein concentrations measured by BCA assay (Pierce).

Macrophage depletion, purification and adoptive transfer

To deplete macrophages, mice were *i.p.* injected with 200 μ L clodronate liposomes (FormuMax, F70101C-N-10). Thioglycollate broth (*i.p.*, 4% in 2 mL, 3 days, Sigma-Aldrich) was used to elicit peritoneal macrophages. To adoptively transfer macrophages, donor peritoneal macrophages (2×10^6 cells, in 1 mL PBS) were *i.v.* transfused to recipient mice 48 h after liposomal ablation. Efficiencies of both depletion and reconstitution were monitored by immunofluorescent staining of liver sections with rat anti-mouse F4/80 mAb (AF647, BioLegend). Mice were then *i.p.* injected with sCD4 (10 mg/kg) 12 h after the adoptive transfer of indicated macrophages. LPS (10 mg/kg) was administered to mice 12 h after sCD4 administration.

Duolink proximity ligation assay (PLA)

Peritoneal macrophages (PM) or BMDM cells (6×10^5) were seeded on a cover slip in a 6-well plate, and serum-starved in OPTI-MEM overnight, LPS or/and sCD4 were then added at the indicated concentrations for 30 min. Cells were then fixed (4% PFA, 4 °C, 15 min), quenched (0.1 M glycine in PBS, 4 °C, 10 min), washed twice with cold PBS. Permeabilization step was applied for detection of cytosolic proteins (saponin solution, #P0095, Beyotime), 30 min). Cells were blocked using Duolink in situ RED starter kit (Sigma, DUO92101-1KT) for 1 h at room temperature. Primary antibodies (1 μ g/mL) targeting MHCII, TLR4, SHP-2, pSHP-2) were used and inter-protein interaction was visualized with probes (DUO92101-1KT, Sigma) that binds to the primary antibodies according to the manufacturer's protocol. Images were captured with DeltaVison microscope (60x, oil; GE), and red fluorescent dots representative of 1 inter-molecular interaction were counted (4 view fields and at least 160 cells) and analyzed with Imaris Software (Oxford Instruments). IgG isotype used as control.

Immunofluorescence staining

Peritoneal macrophages (3×10^5) were seeded on a cover slip in a 6-well plate, and serum-starved overnight in OPTI-MEM before LPS or/and sCD4 were added. Cells were then fixed, quenched and washed as PLA assays, except that 0.25% Triton X-100 was used

for permeabilization, and 1% BSA in PBST for blocking. Primary antibodies against MHCII, TLR4, EEAL, LAPM1, RAB4, RCAS1, and secondary antibodies (Goat anti-Rat Alexa Fluor 647; Donkey anti-Mouse IgG Alexa Fluor 488; Goat anti-Rabbit Alexa Fluor 555) were applied for fluorescent imaging analyses (DeltaVision OMX, 60 x, oil; GE). Green fluorescent dots (10 view fields and at least 10 cells) were counted and analyzed with Imaris Software (Oxford Instruments).

Live cell imaging of lysosomes

RAW264.7 cells (1×10^5) were seeded in a glass bottom dish (35 mm) for 24 h, then transfected with GFP tagged MHC IIA β or MHC IIA β Δ CT. 24 h later, cells were spiked with lysosome tracker for 30 min. Washed and replaced with pre-warmed fresh medium, LPS (500 ng/mL) or LPS plus sCD4 (125 nM) added to cells. Live cell imaging (every 10 s for 20 min) of 4 random view fields were acquired using Olympus SpinSR10 Ixplorer microscope (60x, oil). The size of the lysosome was analyzed by the Surface combined with the automatically tracking objects of interest using the provided algorithms based on Imaris Software (Oxford Instruments).

Multiplex immunohistochemistry

In brief, 3 μ m FFPE sections were deparaffinized in xylene and then rehydrated in 100%, 95%, 90%, 80%, 70% alcohol successively. Antigen unmasking was performed with a preheated epitope retrieval solution (citrate buffer, pH = 6), endogenous peroxidase was inactivated by incubation in 3% H₂O₂ for 20 min. Sections were then pre-incubated with 10% normal goat serum, followed by incubation of primary antibodies overnight (rabbit anti-CD4 antibody (Abcam; ab183685), rabbit anti-F4/80 antibody (CST; #70074)). Next, sections were incubated with the goat anti-rabbit HRP-conjugated secondary antibodies (Abcam; ab214880) for 60 min at room temperature. The antigenic binding sites were visualized by Opal dyes applied to each secondary antibodies. Opal-690 (FP1497001KT) and Opal-570 (FP1488001KT) were from PerkinElmer. Slices were mounted in DAPI fluoromount-G reagent (p0131, Beyotime) and imaging data were obtained with Vectra3 (20x objective, PerkinElmer). Cell-cell interactions were analyzed with Halo Software (Indica Labs).

Statistical analysis

Statistical analysis was performed by using Log-rank (Mantel-Cox) test, Unpaired *t* test and one-way ANOVA with Dunnett's analysis (Graphpad Prism 8). Data are presented as the mean \pm SD. *P*-value < 0.05 was considered statistically significant.

DATA AVAILABILITY

Data that support the findings of this study are available upon reasonable request to the lead contact (H.T.).

ACKNOWLEDGEMENTS

All authors are grateful to Dr. Xue-tao Cao (The Second Military Medical University, Shanghai) for providing MHC II^{-/-} mice, and Dr. Geogee F. Gao (Institute of Microbiology, CAS) for producing recombinant sCD4 at certain stage of this study. Drs. Hai-rong Chen (Institute of Biophysics, CAS) and Ya-ming Jiu (Institut Pasteur of Shanghai) also provided key technical assistance to the study. We also thank Drs. Yang-xin Fu (Tsinghua University) and Lan-juan Li (Zhejiang University) for their inspiring advice. The work was supported in part by grants from Chinese Academy of Sciences (XDB29030301; 153831KYSB20160038; QYZDJ-SSW-SMC026), Shanghai Municipal Science and Technology Major Project (2018SHZDZX05) and NSFC (81530067) to H.T.; Bill & Melinda Gates Foundation, Shenzhen Municipal Science and Technology Innovation Committee (202002073000002) and NSFC (91442127) to Z.Z. National Science and Technology Major Projects of China to H.T. (2020YFC0845900) and S.L. (2018ZX10101004002004); Shanghai Municipal Natural Sciences Foundation to S.L. (19ZR1463100) and H.P. (20SWAQX23-004-002). S.L. is a fellow of Youth Association of Innovation Promotion, CAS.

AUTHOR CONTRIBUTIONS

S.Z., Q.X., L.S., H.P., Q.W., L.L., Y.L., J.W., J.H.W. and S.L. performed the experiments and analyzed the data. M.P., H.X., G.F., S.G. and W.Z. interpreted data; S.L. and H.P. substantively instructed the work. H.T. conceived and drafted the work. All authors have read and approved the article.

ADDITIONAL INFORMATION

Supplementary information The online version contains supplementary material available at <https://doi.org/10.1038/s41392-023-01438-z>.

Competing interests: The authors declare no competing interests.

REFERENCES

- Kawai, T. & Akira, S. Toll-like receptors and their crosstalk with other innate receptors in infection and immunity. *Immunity*. **34**, 637–650 (2011).
- Janeway, C. A. Jr. & Medzhitov, R. Innate immune recognition. *Annu. Rev. Immunol.* **20**, 197–216 (2002).
- Zhao, J. et al. Hyper innate responses in neonates lead to increased morbidity and mortality after infection. *Proc. Natl Acad. Sci. USA*. **105**, 7528–7533 (2008).
- Medzhitov, R. & Janeway, C. A. Jr. Innate immunity: the virtues of a nonclonal system of recognition. *Cell*. **91**, 295–298 (1997).
- Foster, S. L., Hargreaves, D. C. & Medzhitov, R. Gene-specific control of inflammation by TLR-induced chromatin modifications. *Nature* **447**, 972–978 (2007).
- Chen, L. Co-inhibitory molecules of the B7-CD28 family in the control of T-cell immunity. *Nat. Rev. Immunol.* **4**, 336–347 (2004).
- Liew, F. Y., Xu, D., Brint, E. K. & O'Neill, L. A. Negative regulation of toll-like receptor-mediated immune responses. *Nat. Rev. Immunol.* **5**, 446–458 (2005).
- Kim, K. D. et al. Adaptive immune cells temper initial innate responses. *Nat. Med.* **13**, 1248–1252 (2007).
- Zhao, J. et al. Do adaptive immune cells suppress or activate innate immunity? *Trends Immunol.* **30**, 8–12 (2009).
- Guarda, G. et al. T cells dampen innate immune responses through inhibition of NLRP1 and NLRP3 inflammasomes. *Nature* **460**, 269–273 (2009).
- Angus, D. C. & van der Poll, T. Severe sepsis and septic shock. *N. Engl. J. Med.* **369**, 840–851 (2013).
- Martin, M. D., Badovinac, V. P. & Griffith, T. S. CD4 T cell responses and the sepsis-induced immunoparalysis state. *Front. Immunol.* **11**, 1364 (2020).
- van der Poll, T., van de Veerdonk, F. L., Scicluna, B. P. & Netea, M. G. The immunopathology of sepsis and potential therapeutic targets. *Nat. Rev. Immunol.* **17**, 407–420 (2017).
- Hohlstein, P. et al. Prognostic relevance of altered lymphocyte subpopulations in critical illness and sepsis. *J. Clin. Med.* **8**, 353 (2019).
- Sharma, A., Yang, W. L., Matsuo, S. & Wang, P. Differential alterations of tissue T-cell subsets after sepsis. *Immunol. Lett.* **168**, 41–50 (2015).
- Cabrera-Perez, J., Condotta, S. A., Badovinac, V. P. & Griffith, T. S. Impact of sepsis on CD4 T cell immunity. *J. Leukocyte Biol.* **96**, 767–777 (2014).
- Gordon, S. & Taylor, P. R. Monocyte and macrophage heterogeneity. *Nat. Rev. Immunol.* **5**, 953–964 (2005).
- Biggs, J. R. & Zhang, D.-E. *Molecular Pathology (Second Edition)* 299–328 (Elsevier, 2018).
- Maddon, P. J. et al. The isolation and nucleotide sequence of a cDNA encoding the T cell surface protein T4: a new member of the immunoglobulin gene family. *Cell* **42**, 93–104 (1985).
- Cammarota, G. et al. Identification of a CD4 binding site on the beta 2 domain of HLA-DR molecules. *Nature* **356**, 799–801 (1992).
- Forsgren, S., Pobor, G., Coutinho, A. & Pierres, M. The role of I-A/E molecules in B lymphocyte activation. I. Inhibition of lipopolysaccharide-induced responses by monoclonal antibodies. *J. Immunol.* **133**, 2104–2110 (1984).
- Rodo, J. et al. MHC class II molecules control murine B cell responsiveness to lipopolysaccharide stimulation. *J. Immunol.* **177**, 4620–4626 (2006).
- Gossez, M. et al. Proof of concept study of mass cytometry in septic shock patients reveals novel immune alterations. *Sci. Rep.* **8**, 17296 (2018).
- Girardot, T., Rimmel, T., Venet, F. & Monneret, G. Apoptosis-induced lymphopenia in sepsis and other severe injuries. *Apoptosis* **22**, 295–305 (2017).
- Li, H. et al. SARS-CoV-2 and viral sepsis: observations and hypotheses. *Lancet* **395**, 1517–1520 (2020).
- Pedersen, S. F. & Ho, Y. C. SARS-CoV-2: a storm is raging. *J. Clin. Investig.* **130**, 2202–2205 (2020).
- Platt, E. J. et al. Effects of CCR5 and CD4 cell surface concentrations on infections by macrophagetropic isolates of human immunodeficiency virus type 1. *J. Virol.* **72**, 2855–2864 (1998).

28. Orozco, S. L., Canny, S. P. & Hamerman, J. A. Signals governing monocyte differentiation during inflammation. *Curr. Opin. Immunol.* **73**, 16–24 (2021).
29. Delneste, Y. et al. Interferon-gamma switches monocyte differentiation from dendritic cells to macrophages. *Blood* **101**, 143–150 (2003).
30. Zanoni, I. et al. CD14 controls the LPS-induced endocytosis of Toll-like receptor 4. *Cell* **147**, 868–880 (2011).
31. McDevitt, H. O. Discovering the role of the major histocompatibility complex in the immune response. *Annu. Rev. Immunol.* **18**, 1–17 (2000).
32. Al-Daccak, R., Mooney, N. & Charron, D. MHC class II signaling in antigen-presenting cells. *Curr. Opin. Immunol.* **16**, 108–113 (2004).
33. Zhao, Y. et al. Publisher correction: SARS-CoV-2 spike protein interacts with and activates TLR4. *Cell Res.* **31**, 825 (2021).
34. Inoue, M. et al. T cells down-regulate macrophage TNF production by IRAK1-mediated IL-10 expression and control innate hyperinflammation. *Proc. Natl Acad. Sci. USA.* **111**, 5295–5300 (2014).
35. Kawai, T. & Akira, S. The role of pattern-recognition receptors in innate immunity: update on Toll-like receptors. *Nat. Immunol.* **11**, 373–384 (2010).
36. Kissner, T. L. et al. Activation of MyD88 signaling upon staphylococcal enterotoxin binding to MHC class II molecules. *PLoS One* **6**, e15985 (2011).
37. Li, W. et al. STK4 regulates TLR pathways and protects against chronic inflammation-related hepatocellular carcinoma. *J. Clin. Invest.* **125**, 4239–4254 (2015).
38. Yamin, T. T. & Miller, D. K. The interleukin-1 receptor-associated kinase is degraded by proteasomes following its phosphorylation. *J. Biol. Chem.* **272**, 21540–21547 (1997).
39. O'Neill, L. A. When signaling pathways collide: positive and negative regulation of toll-like receptor signal transduction. *Immunity* **29**, 12–20 (2008).
40. Xu, S. et al. Constitutive MHC class I molecules negatively regulate TLR-triggered inflammatory responses via the Fps-SHP-2 pathway. *Nat. Immunol.* **13**, 551–559 (2012).
41. Harton, J., Jin, L., Hahn, A. & Drake, J. Immunological functions of the membrane proximal region of MHC class II molecules. *F1000Res* **5**, 368–379 (2016).
42. Zhang, C. et al. Structural basis of STING binding with and phosphorylation by TBK1. *Nature* **567**, 394–398 (2019).
43. Plociennikowska, A., Hromada-Judycka, A., Borzecka, K. & Kwiatkowska, K. Co-operation of TLR4 and raft proteins in LPS-induced pro-inflammatory signaling. *Cell. Mol. Life Sci.* **72**, 557–581 (2015).
44. Brodsky, F. M. Antigen processing and presentation: close encounters in the endocytic pathway. *Trends Cell Biol.* **2**, 109–115 (1992).
45. Cella, M. et al. Inflammatory stimuli induce accumulation of MHC class II complexes on dendritic cells. *Nature* **388**, 782–787 (1997).
46. Cho, K. J., Walseng, E., Ishido, S. & Roche, P. A. Ubiquitination by March-I prevents MHC class II recycling and promotes MHC class II turnover in antigen-presenting cells. *Proc. Natl Acad. Sci. USA.* **112**, 10449–10454 (2015).
47. Zhong, G., Romagnoli, P. & Germain, R. N. Related leucine-based cytoplasmic targeting signals in invariant chain and major histocompatibility complex class II molecules control endocytic presentation of distinct determinants in a single protein. *J. Exp. Med.* **185**, 429–438 (1997).
48. Garcia, K. C. Insights into immune structure, recognition, and signaling. *Immunol. Rev.* **250**, 5–9 (2012).
49. Doyle, C. & Strominger, J. L. Interaction between CD4 and class II MHC molecules mediates cell adhesion. *Nature* **330**, 256–259 (1987).
50. Harton, J. A. Class II MHC cytoplasmic domain-mediated signaling in B cells: A tail of two signals. *Hum. Immunol.* **80**, 32–36 (2019).
51. Nagy, Z. A. et al. Fully human, HLA-DR-specific monoclonal antibodies efficiently induce programmed death of malignant lymphoid cells. *Nat. Med.* **8**, 801–807 (2002).
52. Setterblad, N. et al. Cognate MHC-TCR interaction leads to apoptosis of antigen-presenting cells. *J. Leukoc. Biol.* **75**, 1036–1044 (2004).
53. Bertho, N. et al. HLA-DR-mediated apoptosis susceptibility discriminates differentiation stages of dendritic/monocytic APC. *J. Immunol.* **164**, 2379–2385 (2000).
54. McLellan, A. D. et al. Differential susceptibility to CD95 (Apo-1/Fas) and MHC class II-induced apoptosis during murine dendritic cell development. *Cell Death Differ.* **7**, 933–938 (2000).
55. Longo, D. L. DR's orders: human antibody kills tumors by direct signaling. *Nat. Med.* **8**, 781–783 (2002).
56. Jin, L. et al. MPYS, a novel membrane tetraspanner, is associated with major histocompatibility complex class II and mediates transduction of apoptotic signals. *Mol. Cell. Biol.* **28**, 5014–5026 (2008).
57. Tang, H. & Fu, Y. A new role for T cells in dampening innate inflammatory responses. *Sci. China Life Sci.* **53**, 190–194 (2010).
58. Sun, Y. et al. B and T lymphocyte attenuator tempers early infection immunity. *J. Immunol.* **183**, 1946–1951 (2009).
59. Lokshin, A. E. et al. Differential regulation of maturation and apoptosis of human monocyte-derived dendritic cells mediated by MHC class II. *Int. Immunol.* **14**, 1027–1037 (2002).
60. Scholl, P. R. & Geha, R. S. MHC class II signaling in B-cell activation. *Immunol. Today* **15**, 418–422 (1994).
61. Scholl, P. R., Trede, N., Chatila, T. A. & Geha, R. S. Role of protein tyrosine phosphorylation in monokine induction by the staphylococcal superantigen toxic shock syndrome toxin-1. *J. Immunol.* **148**, 2237–2241 (1992).
62. Andraea, S., Buisson, S. & Triebel, F. MHC class II signal transduction in human dendritic cells induced by a natural ligand, the LAG-3 protein (CD223). *Blood* **102**, 2130–2137 (2003).
63. Dong, G. et al. STING Negatively Regulates Double-Stranded DNA-Activated JAK1-STAT1 Signaling via SHP-1/2 in B Cells. *Mol. Cells* **38**, 441–451 (2015).
64. Ouyang, S. et al. Structural analysis of the STING adaptor protein reveals a hydrophobic dimer interface and mode of cyclic di-GMP binding. *Immunity* **36**, 1073–1086 (2012).
65. Dal Porto, J. M. et al. B cell antigen receptor signaling 101. *Mol. Immunol.* **41**, 599–613 (2004).
66. Kim, E. J., Lee, S. M., Suk, K. & Lee, W. H. CD300a and CD300f differentially regulate the MyD88 and TRIF-mediated TLR signalling pathways through activation of SHP-1 and/or SHP-2 in human monocytic cell lines. *Immunology* **135**, 226–235 (2012).
67. Liu, X. et al. Intracellular MHC class II molecules promote TLR-triggered innate immune responses by maintaining activation of the kinase Btk. *Nat. Immunol.* **12**, 416–424 (2011).
68. Tseng, W. Y. et al. Increased soluble CD4 in serum of rheumatoid arthritis patients is generated by matrix metalloproteinase (MMP)-like proteinases. *PLoS One* **8**, e63963 (2013).
69. Xiong, Y., Kern, P., Chang, H. & Reinherz, E. T cell receptor binding to a pMHCII ligand is kinetically distinct from and independent of CD4. *J. Biol. Chem.* **276**, 5659–5667 (2001).
70. Baue, A. E. Sepsis research: what did we do wrong? What would Semmelweis do today? *Shock* **16**, 1–8 (2001).
71. Rittirsch, D., Huber-Lang, M. S., Flierl, M. A. & Ward, P. A. Immunodesign of experimental sepsis by cecal ligation and puncture. *Nat. Protoc.* **4**, 31–36 (2009).
72. He, X. et al. Bap180/Baf180 is required to maintain homeostasis of intestinal innate immune response in Drosophila and mice. *Nat. Microbiol.* **2**, 17056 (2017).



Open Access This article is licensed under a Creative Commons Attribution 4.0 International License, which permits use, sharing, adaptation, distribution and reproduction in any medium or format, as long as you give appropriate credit to the original author(s) and the source, provide a link to the Creative Commons license, and indicate if changes were made. The images or other third party material in this article are included in the article's Creative Commons license, unless indicated otherwise in a credit line to the material. If material is not included in the article's Creative Commons license and your intended use is not permitted by statutory regulation or exceeds the permitted use, you will need to obtain permission directly from the copyright holder. To view a copy of this license, visit <http://creativecommons.org/licenses/by/4.0/>.

© The Author(s) 2023